Waikato Regional Council Technical Report 2020/05

Ground penetrating radar survey of buried sinter at Armstrong Reserve, Waipahihi

www.waikatoregion.govt.nz
ISSN 2230-4355 (Print)
ISSN 2230-4363 (Online)

Waikato
REGIONAL COUNCIL
Te Kaunihera ā Rohe o Waikato

Prepared by:
Bridget Lynne, Isaac J Smith and Gary J Smith (Geothermal Scientific Investigations Ltd)

For:
Waikato Regional Council
Private Bag 3038
Waikato Mail Centre
HAMILTON 3240

June 2020

Document #: 16217084

Peer reviewed by:
Katherine Luketina Date June 2020

Approved for release by:
Mike Scarsbrook Date June 2020

Disclaimer

This technical report has been prepared for the use of Waikato Regional Council as a reference document and as such does not constitute Council's policy.

Council requests that if excerpts or inferences are drawn from this document for further use by individuals or organisations, due care should be taken to ensure that the appropriate context has been preserved, and is accurately reflected and referenced in any subsequent spoken or written communication.

While Waikato Regional Council has exercised all reasonable skill and care in controlling the contents of this report, Council accepts no liability in contract, tort or otherwise, for any loss, damage, injury or expense (whether direct, indirect or consequential) arising out of the provision of this information or its use by you or any other party.

Table of Contents

Abstract

Ground Penetrating Radar (GPR) was undertaken over the southern section of the Armstrong Reserve, located in Taupo, New Zealand, to image the shallow subsurface. Historically, hot springs were located in this area. These springs discharged silica-rich, alkali-chloride water resulting in the formation of siliceous sinter terraces. No discharging hot springs are visible at the site today, although the historic sinter is exposed along the banks of a stream that dissects the study area. This stream is fed by thermal springs further upstream. GPR was used to image the buried sinter and to identify fractures within the sinter. The GPR data revealed three distinctive rock types in the subsurface; (1) unaltered siliceous sinter producing strong GPR reflections, (2) Rock Type B consisting of a poorly-reflective unit, (3) Rock Type C producing discontinuous horizons of strong reflections mixed with zones of poorly-reflective material. Fractures within the subsurface were also identified. GPR data was collected to a depth of eight metres along thirty-eight transect lines. Transects were arranged in a grid system to enable 3D modelling of the subsurface.

Geothermal Scientific Investigations Ltd.

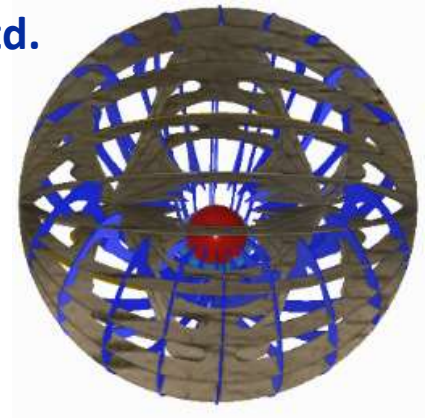

Ground Penetrating Radar report of Armstrong Reserve, Taupo, New Zealand

April 2016

1 Introduction

The Taupo area lies within the Taupo Volcanic Zone (TVZ) and is well-known for its thermal activity (Rosenberg et al., 2010). The Armstrong Reserve is located on the northern shores of Lake Taupo with the Onekeneke Stream dissecting the Armstrong Reserve (Figures 1, 2). Historic hot spring rocks referred to as siliceous sinter are present underneath the grassed area at Armstrong Reserve and are exposed along the banks of the Onekeneke Stream. Thermal input to the Onekeneke Stream occurs further upstream. Currently there are no discharging hot springs at the study site. At the time of the survey the temperature of the Onekeneke Stream 21.7 °C and the pH was 8.5.

A Ground Penetrating Radar survey of the western area of the Armstrong Reserve was undertaken in April 2016. GPR is a high-resolution geophysical tool that is used to image the shallow subsurface. Siliceous sinters image particularly well using GPR as they produce strong amplitude reflections (Dougherty and Lynne, 2011; Lynne and Sim, 2012; Lynne and Smith, 2013: Lynne et al., 2015). The aim of this study was to identify the lateral and vertical distribution of the buried sinter and any fractures present within the sinter.

2 Objectives

1) Collect Ground Penetrating Radar (GPR) data at Armstrong Reserve to see if buried sinter can be imaged. Determine if fractures are present within the sinter.

2a) If the area adjacent to and inside culvert 1 is dry at the time of the survey, it will be assessed for subsurface fractures using GPR.

2b) GPR will be used to image the shallow subsurface to establish if any fractures are present in the sinter terrace near culvert 2 which could be allowing the stream water to flow beneath culvert 2.

3 Site Information

A GPR survey was conducted at the Armstrong Reserve in Taupo, New Zealand (Fig. 1) in April 2016. The Armstrong Reserve is covered in grass, with a thermal stream known as the Onekeneke Stream dissecting the grassed area. At the time of the survey, the stream was flowing and had a temperature of 21.7°C and a pH of 8.56. In the banks of the stream, sinter was identified at several locations. The area is known for its historic siliceous sinters. Figures 2 to 5 show the location of the 38 individual GPR transect lines.

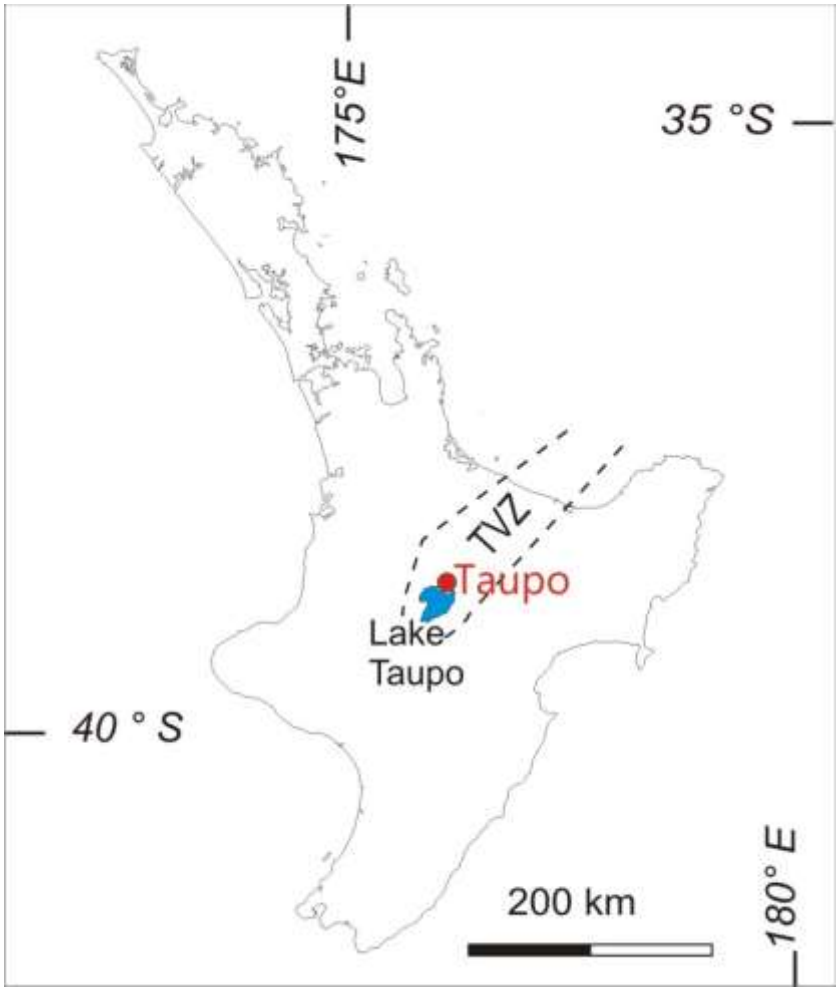

Figure 1: Location map of Taupo within the Taupo Volcanic Zone (TVZ), New Zealand.

Figure 2: Overview of all GPR transect lines and their distribution at Armstrong Reserve.

Figure 3: Overview of the western section of the study area showing individual GPR transect lines.

Figure 4: Overview of the eastern section of the study area showing individual GPR transect lines.

Figure 5: Location of transect 038 over the western-most culvert.

4 Field Work

The Armstrong Reserve field work was conducted during dry weather in April 2016. Rainfall occurred 24 hours prior to the commencement of the field work. Therefore, the subsurface may have been semi-saturated during the time of the GPR survey. Groundwater has a distinctive effect on the GPR waveform and the resulting processed image. Due to the GPR wave speed slowing down when travelling through water, some strong sinter reflectors at depth in zones of fluid retention will appear faded, but are still distinctive. Only one of the two culverts in the study area could be surveyed. A GPR survey of the eastern-most culvert (1) and its surrounding outflow apron could not be undertaken due to surface water flow in these areas. A total of 38 transects were collected and processed.

5 Methods

The GPR survey was undertaken using a Sir 3000 control unit with a 200MHz Antenna. Estimated maximum depth imaged at this site is 8 m. The colour scale view used in this report has been chosen to easily identify highly-reflective substrates, such as siliceous sinter. Poor reflectors such as soil appear as black areas in the colour images.

6 Image Interpretation

Both colour and grayscale images of each transect are presented in this report. Both images are identical apart from the colour scheme (Fig. 6). It is important to note that the sub-surface classifications shown in Figure 6 apply to all the GPR images in the report. As with all geophysical methods the classification cannot be fully confirmed without ground-truthing the area.

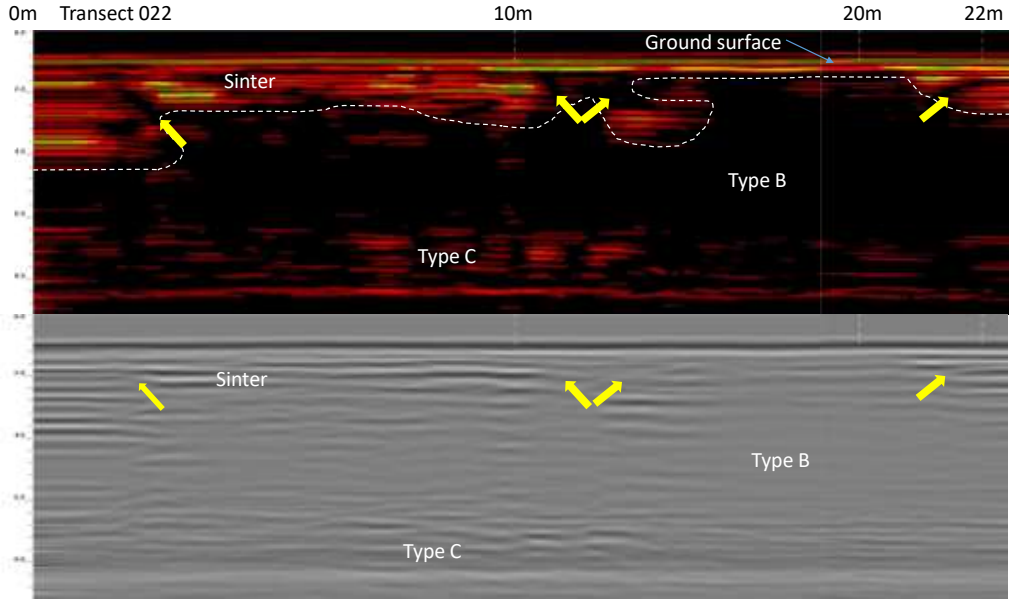

Figure 6: Example of grayscale and colour GPR images with sinter and Types B and C units shown. Yellow arrows infer potential fractures.

Colour GPR images: The colour range has been selected as it highlights differences between strong and weak reflectors. In the colour images, white indicates sites where the reflectors were the strongest. Blues and purples are moderately-strong reflectors. Red/yellow/green indicates sites of moderate signal return. Black denotes a poor reflector.

Grayscale GPR images: Grayscale images are the original colour scheme which shows the data with no filter. These images highlight buried structures, such as pipes. Strong reflectors are

shown as gray and white strips. Moderate reflectors produce hazy or blurry pale gray and white striped areas. Weak reflectors produce pale gray zones with no stripes.

Classifications used in this study

Ground surface: The thick horizontal line just below the 0 m mark is the ground surface, and with the exception of the above image, it will not be labelled in this report.

Sinter: Unaltered siliceous sinter produces strong GPR reflections. Altered sinters produce moderate to weak reflections depending on the degree of alteration. Saturated sinter produces moderate to weak reflections depending on the amount of saturation.

Fractures: Subsurface fractures image as black areas (yellow arrows). The orientation of the arrow approximately matches the fracture orientation.

Type B: Unidentified, poorly-reflective material. Most likely to be soil, clay or water saturated regolith.

Type C: Likely to be discontinuous sinter horizons due to fracturing, hydrothermal alteration, incorporation of soil or sediments, or steam/water infilling fractures or voids.

7 Results

Presented in the results section are the GPR profiles of individual transects. Transect location photographs are provided in Appendix A.

7.1 Transect 005

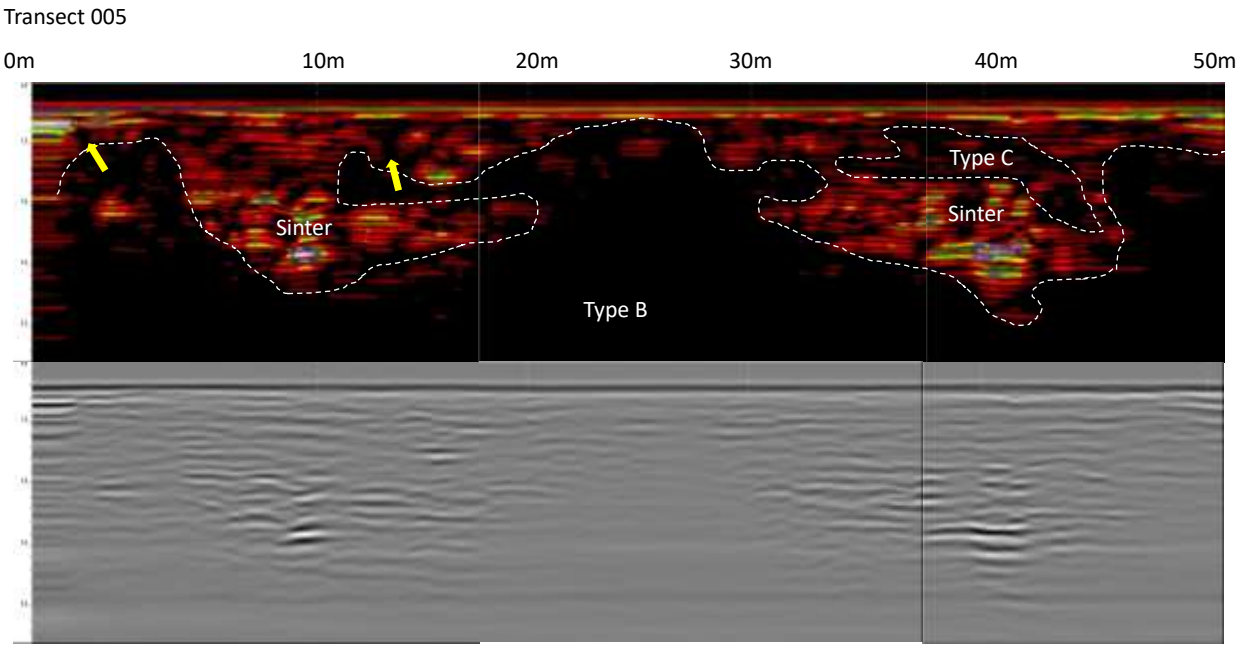

Figure 7: Transect 005. 50 m transect line showing discontinuous, horizontal, sinter layers along the entire transect. Sinter thickness varies from ~1 m to 6 m. Two fractures occur at ~2 and 12 m. Both fractures have similar orientations.

7.2 Transect 006

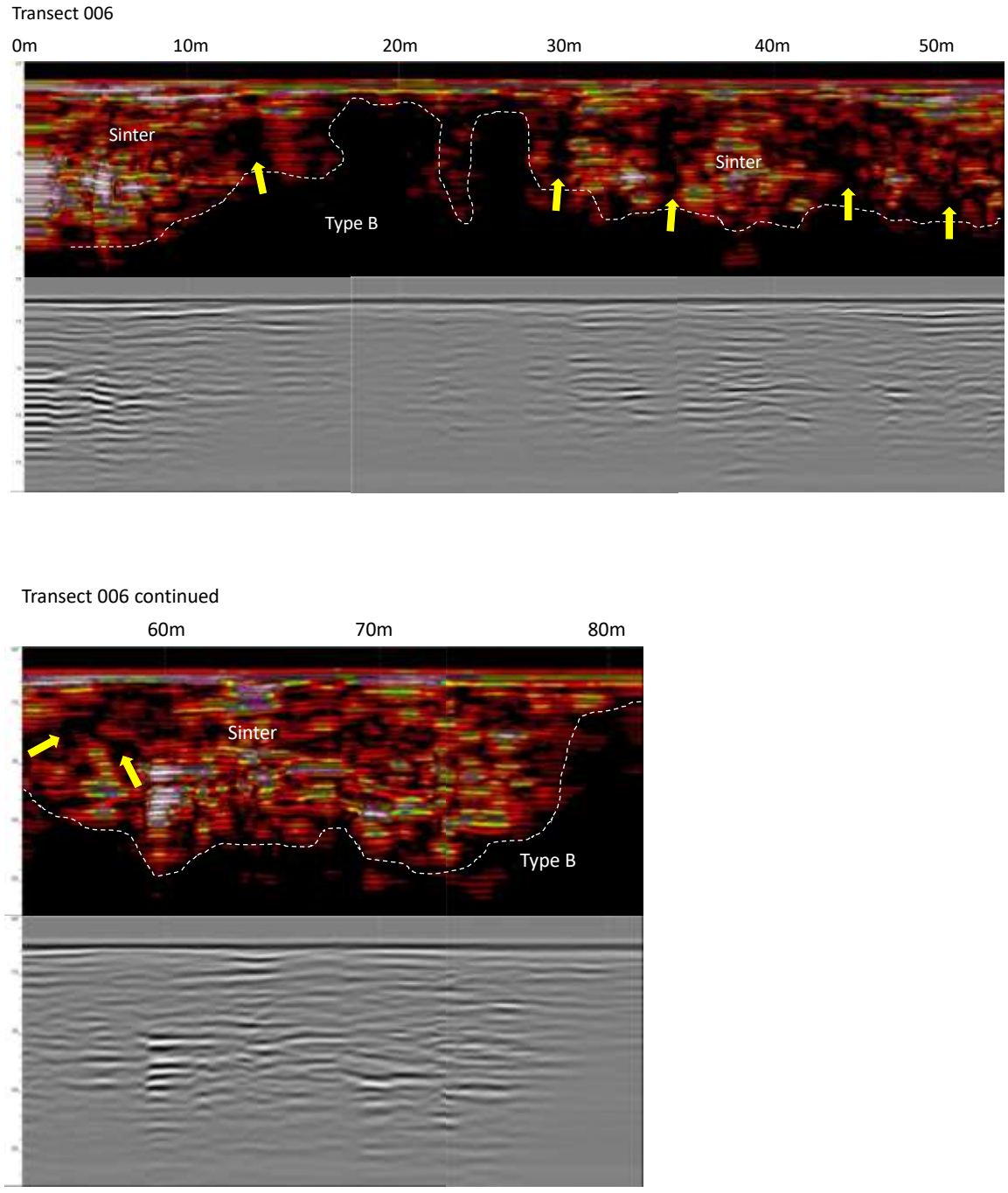

Figure 8: Transect 006. 80 m profile line showing thick, sinter between 0 to 18 m and 28 to 80 m. Sinter varies in thickness from 1 to 8 m. Multiple, fractures with near-vertical orientations (yellow arrows). Type B occurs in varying thickness underneath the sinter.

7.3 Transect 007

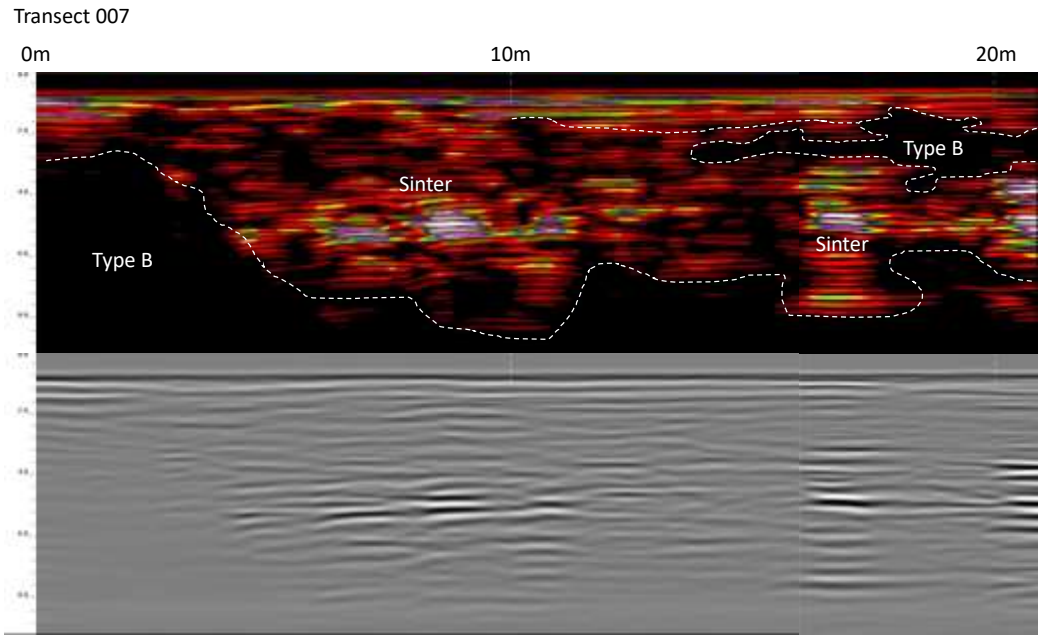

Figure 9: Transect 007. 20 m profile line. Sinter thickens between 0 and 5 m, with thick (up to ~ 8 m) horizontal sinter layers from 5 to 20 m.

7.4 Transect 008

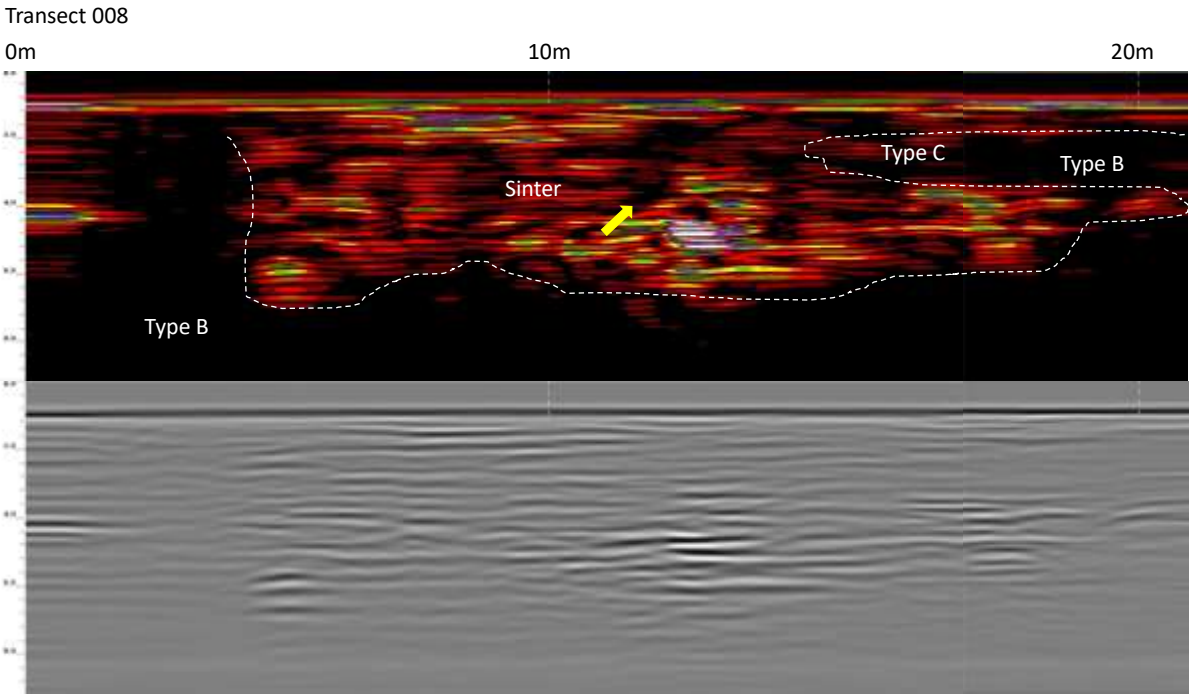

Figure 10: Transect 008. 20 m transect line. Sharp, abrupt contact between Type B and sinter at the 4 m mark. Horizontal sinter sheets, up to 7 m thick were imaged between 4 and 20 m, with a fracture at 12 m (yellow arrow). Sinter is interbedded with Types B and C between the 15 to 20 m marks.

7.5 Transect 009

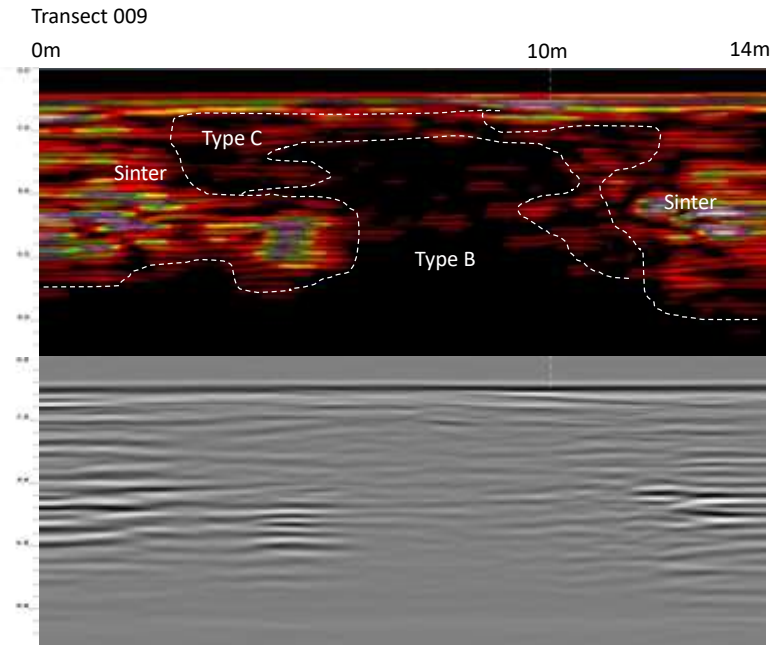

Figure 11: Transect 009. 14 m profile line shows two pockets of sinter separated by ~5 m of Type B and Type C material. Sinter layers are dominantly horizontal with slight lateral variations in radar signal return indicating a variation in properties across the layers.

7.6 Transect 010

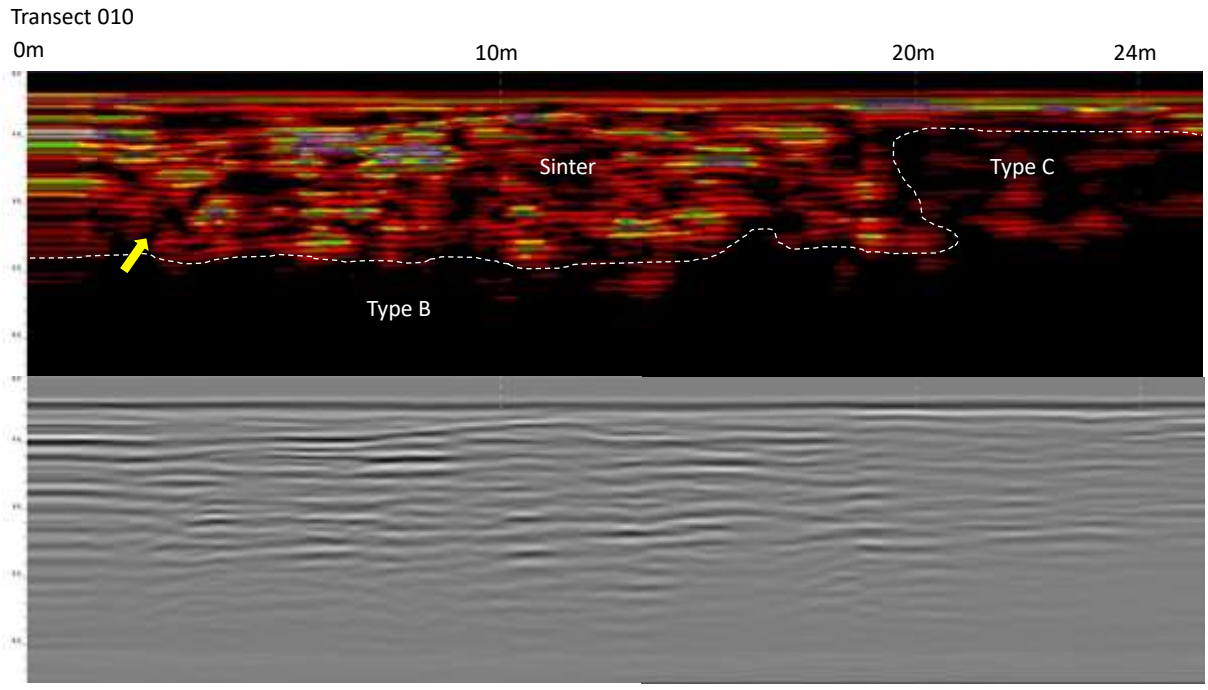

Figure 12: Transect 010. A 24 m long profile line showing sinter horizons between 0 and 20 m to a depth of ~6 m. From 20 to 24 m the sinter thins to ~ 1 m and Type C dominates this zone. Sinter layers are fractured (yellow arrow). Type B is present below the sinter.

7.7 Transect 011

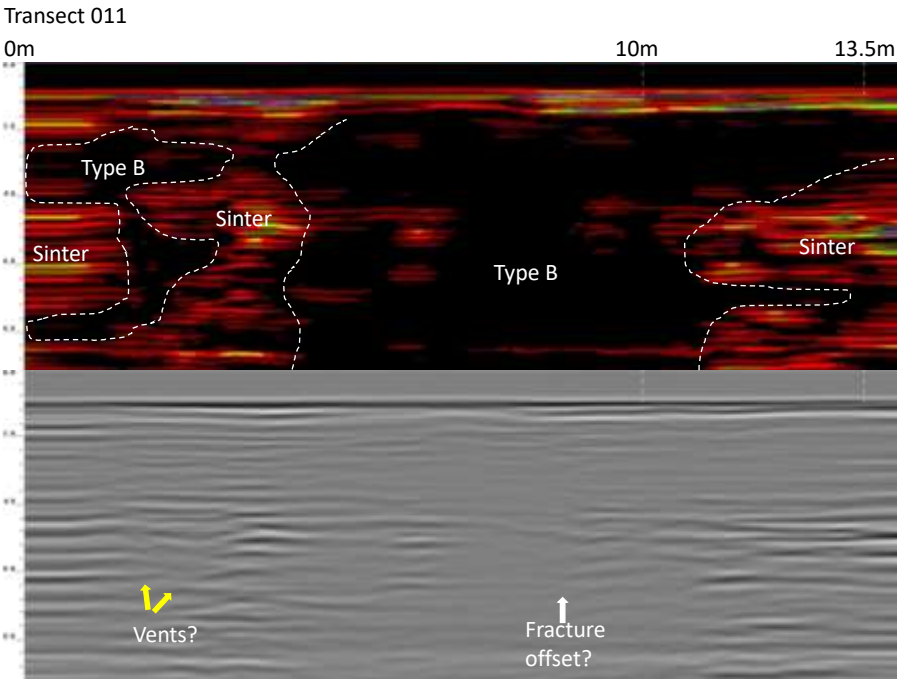

Figure 13: Transect 011. 13.5 m transect line with areas of sinter separated by a ~6 m band of Type B material. Sinter thickness varies and not all the sinter reaches the surface. There are faint signatures which could represent vents and a fracture offset, as shown on the image.

7.8 Transect 012

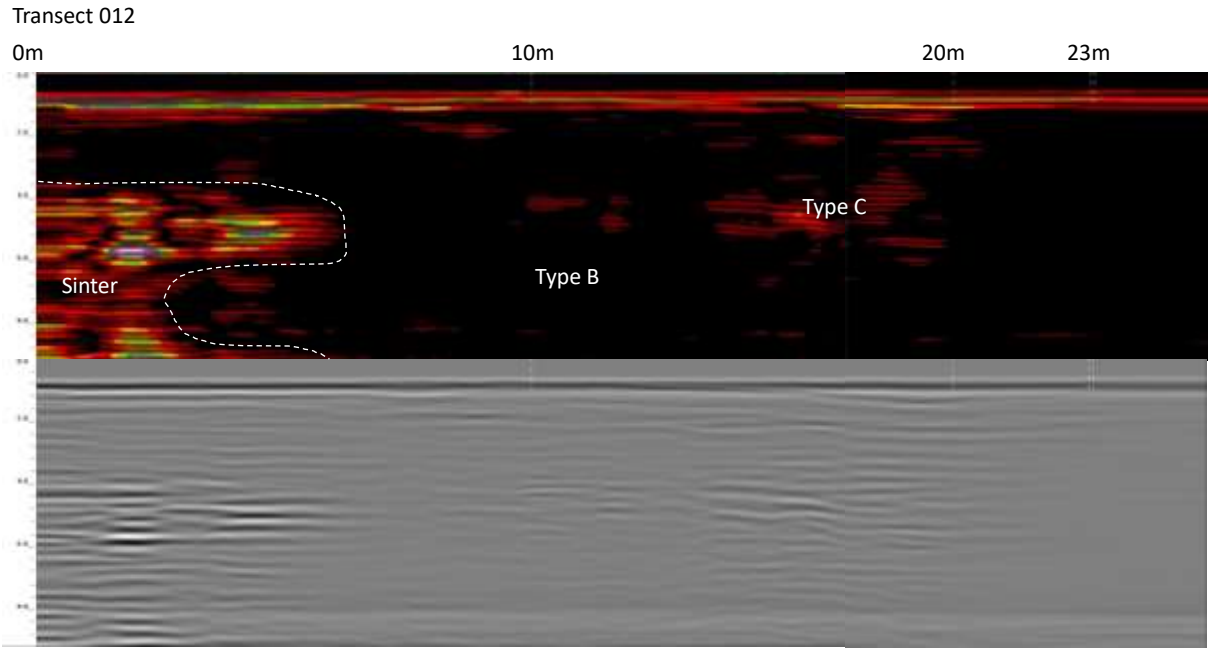

Figure 14: Transect 012. 23 m transect line dominated by Type B with minor Type C at 15-17 m. A pocket of sinter occupies the first 5 m of the profile but does not reach the surface.

7.9 Transect 013

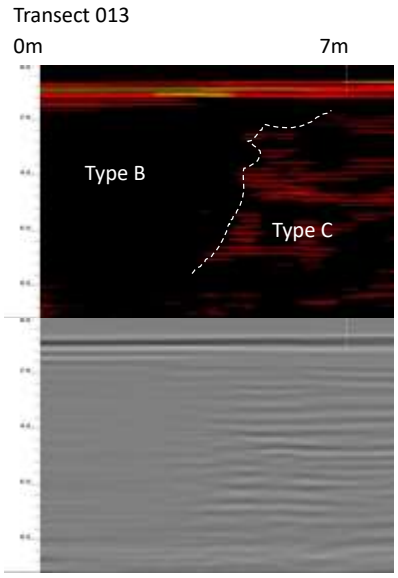

Figure 15: Transect 013. 7 m long profile that revealed no strong sinter reflectors in this area. Type B spans the first 3.5 m and Type C was imaged from 3.5 m to 7 m.

7.10 Transect 014

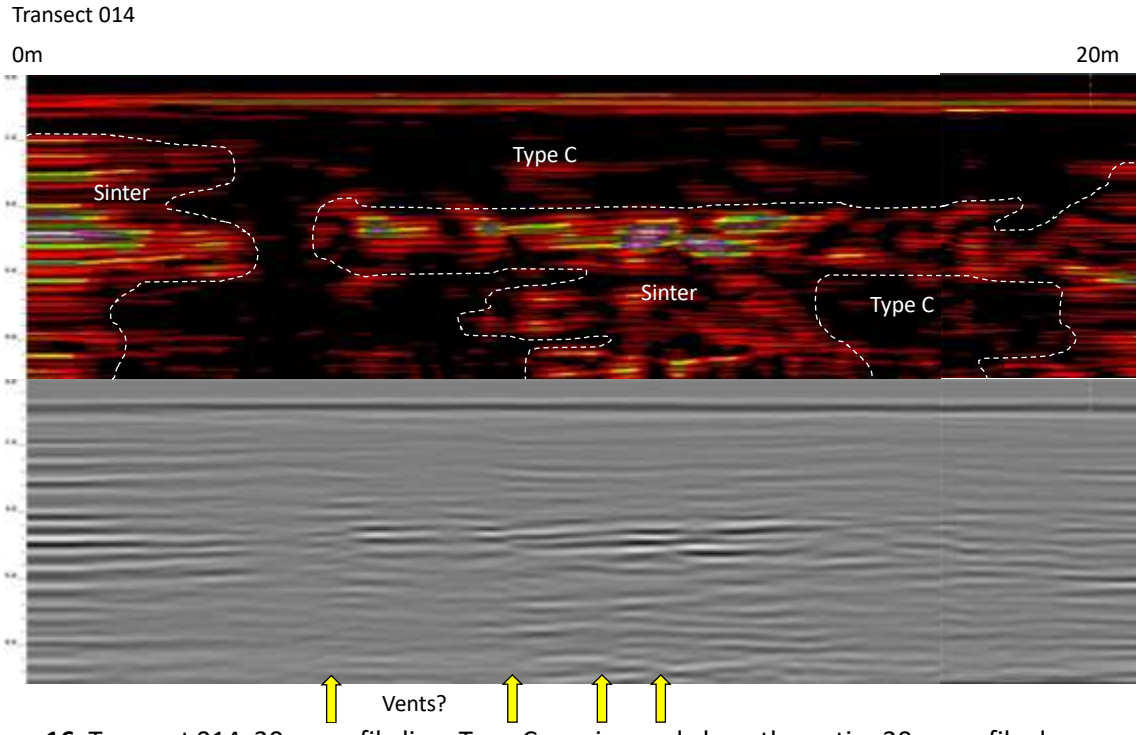

Figure 16: Transect 014. 20 m profile line. Type C was imaged along the entire 20 m profile down to depths of 1 to 8 m. Two zones of sinter were imaged at 0 to 3 m and 5 to 20 m along the transect. Both the sinter zones are buried below Type C material. Sinter thickness varies. There are four possible vents located (yellow arrows) within the 5 to 15 m band of the transect.

7.11 Transect 015

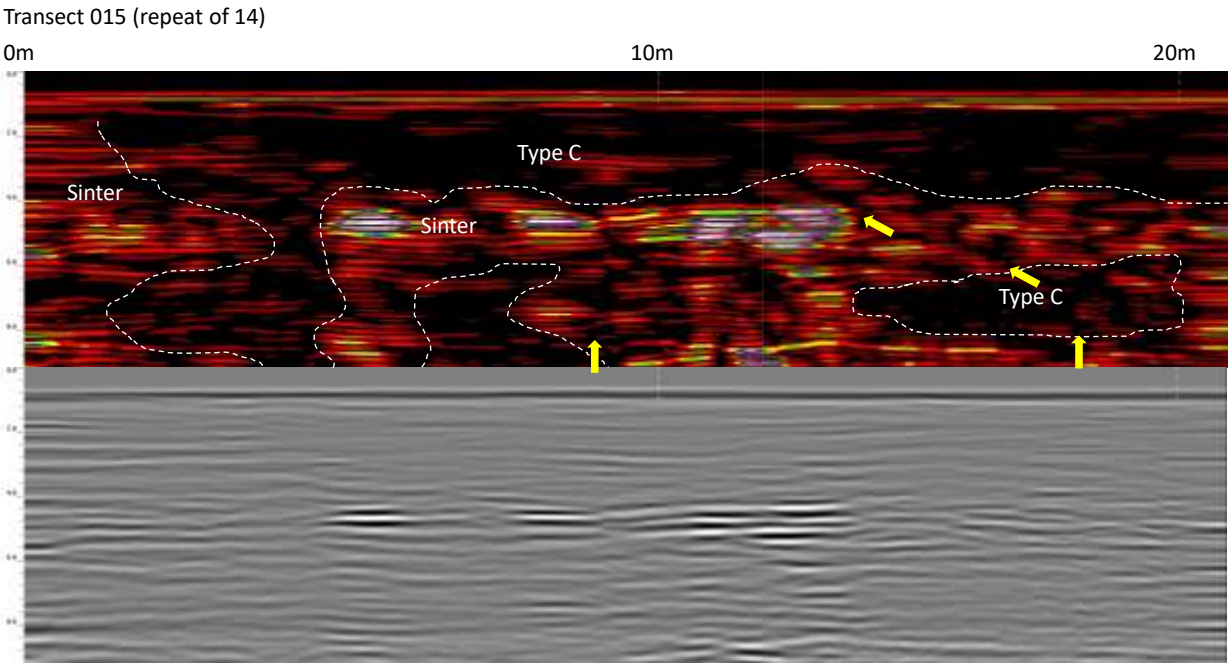

Figure 17: Transect 015. 20 m profile line. A 15 m long, discontinuous zone of sinter at 4 m depth is overlain and enclosed by Type C. Sinter also occurs immediately below the ground surface at the start of the transect line to a depth of ~ 8 m. Larger vents shown by yellow arrows.

7.12 Transect 016

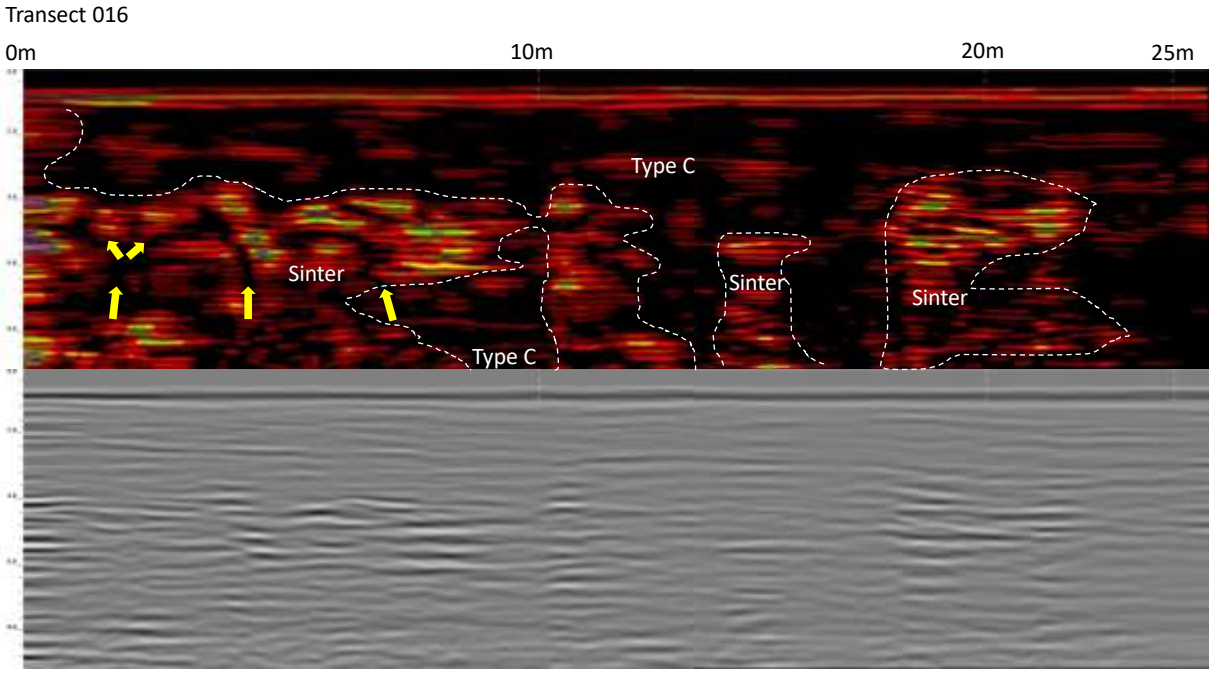

Figure 18: Transect 016. 25 m profile line. Discontinuous sinter at 4 m depth with Type C overlying and dispersed amongst the sinter. Vents shown by yellow arrows. The left most vent splits into two fracture pathways below the surface at the 4.5 m mark.

7.13 Transect 017

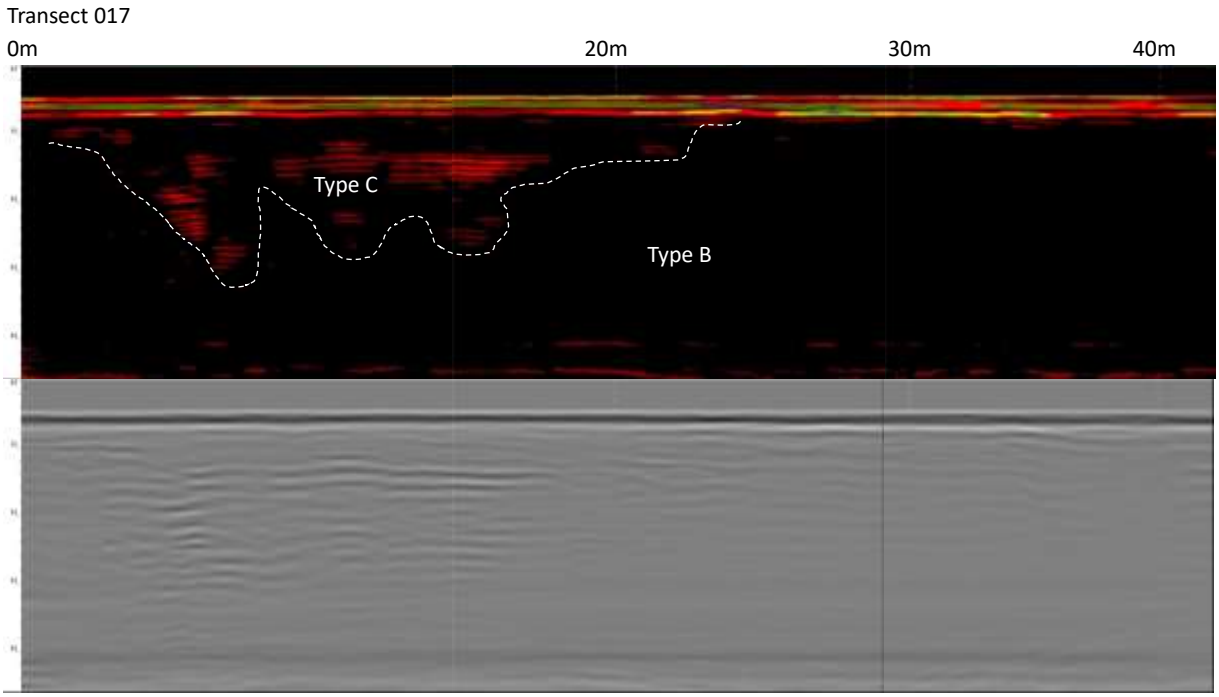

Figure 19: Transect 017. 40 m transect line. Type C is present between 0 and 20 m, varying from ~1 to 4 m depth. Type B occurs between 25 and 40 m at the surface and underneath Type C from 0 to 25 m.

7.14 Transect 018

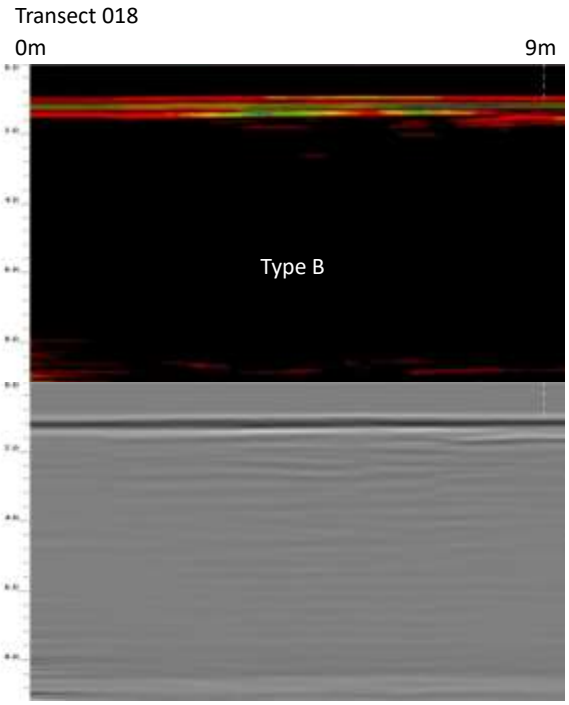

Figure 20: Transect 018. 9 m long profile showing Type B material.

7.15 Transect 019

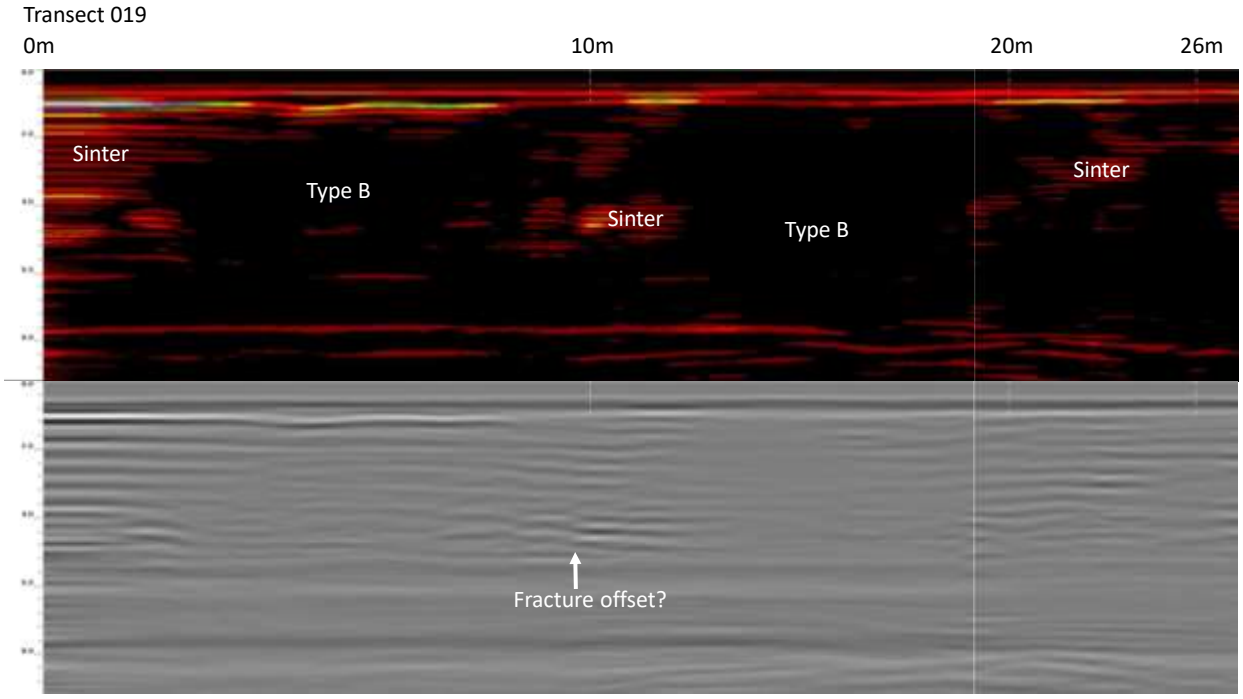

Figure 21: Transect 019. 26 m long profile. Small, isolated pockets of sinter roughly 2 m in diameter to ~4 m depth, are surrounded by Type B material. There is a potential fracture offset at 10 m.

7.16 Transect 020

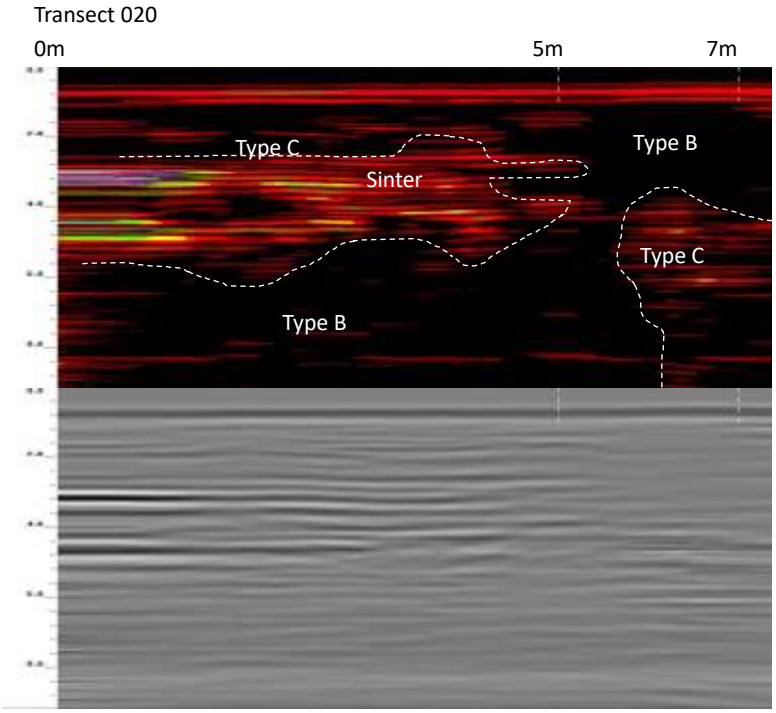

Figure 22: Transect 020. 7 m profile line. Horizontal sinter sheets are present at ~3 to 6 m depth and extend horizontally for 5 m. The sinter is surrounded by Type B and Type C material.

7.17 Transect 021

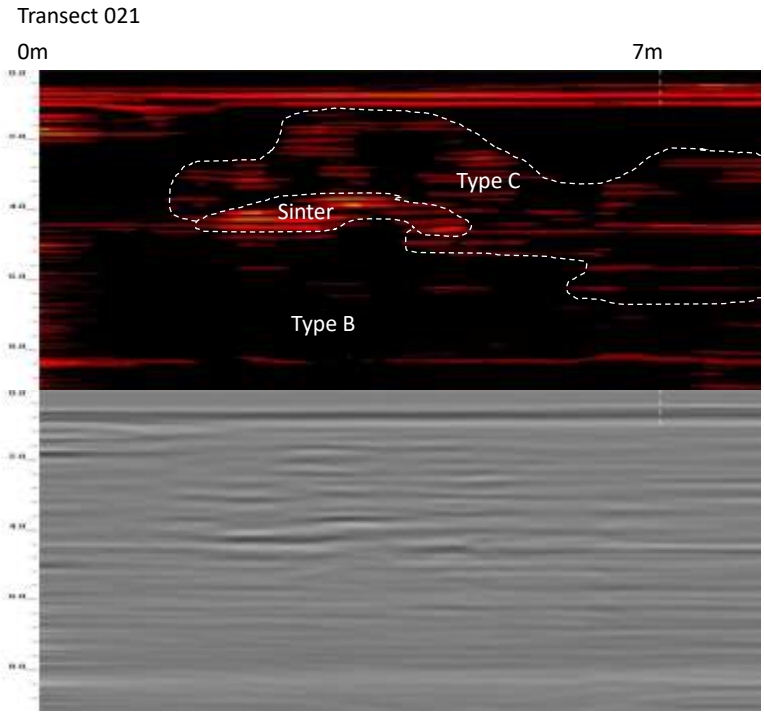

Figure 23: Transect 021. 7 m transect line. Dominantly Type B. At the 2 to 5 m mark and at 4 m depth, there is a 3 m long x ~1 m thick layer of sinter.

7.18 Transect 022

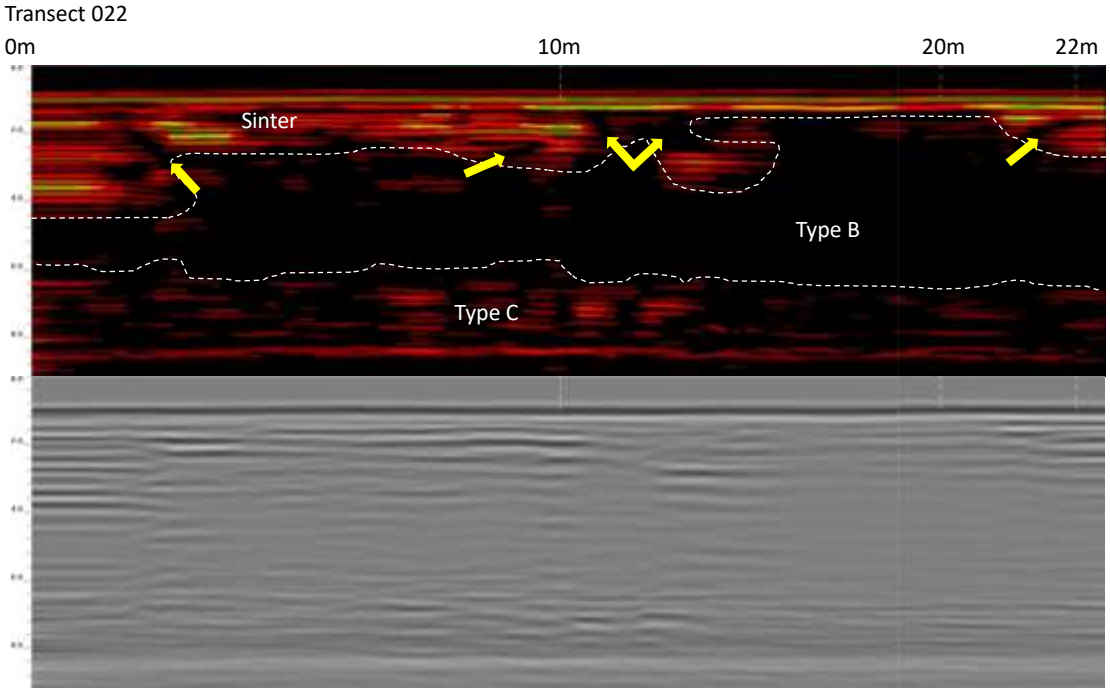

Figure 24: Transect 022. 22 m long profile. Sinter is present at or just below the surface of this transect, extending along the majority of the 22 m profile line to a maximum depth of ~4 m. Immediately below this sinter layer is a horizontally, continuous section of Type B to approximately 6 m depth. From 6 to 8 m depth Type C is present. Yellow arrows show multiple fractures with varying orientations.

7.19 Transect 023

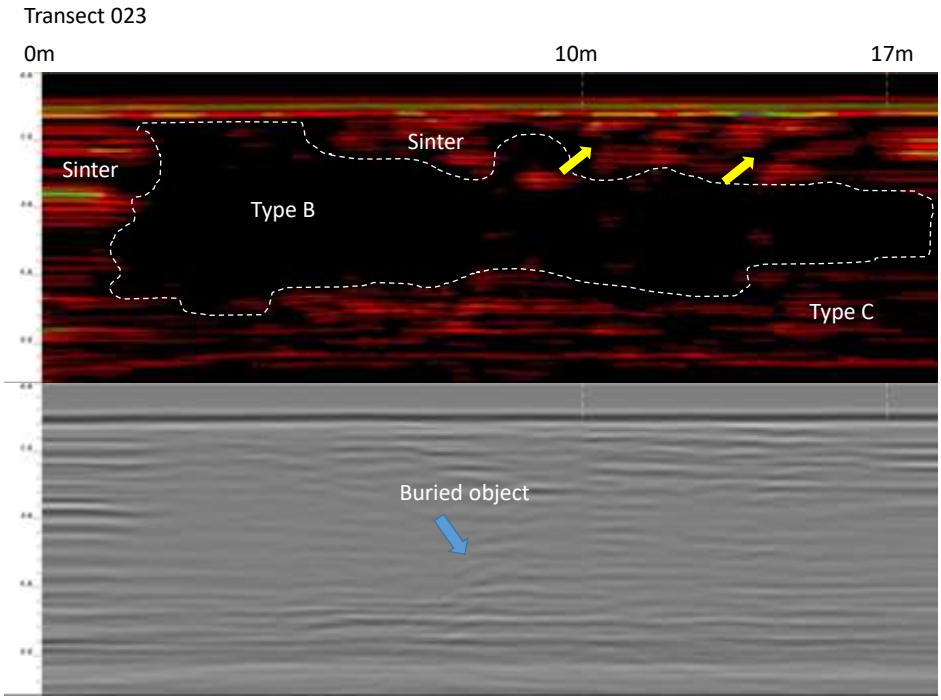

Figure 25: Transect 023. 17 m transect line. Sinter is present at 1 to 5 m depth from the 0 to 2 m mark and then continues between 6 and 17 m with a pocket of Type B below the sinter. Type C is present at 6 to 8 m depth across the extent of the profile. A buried object was encountered at ~9 m.

7.20 Transect 024

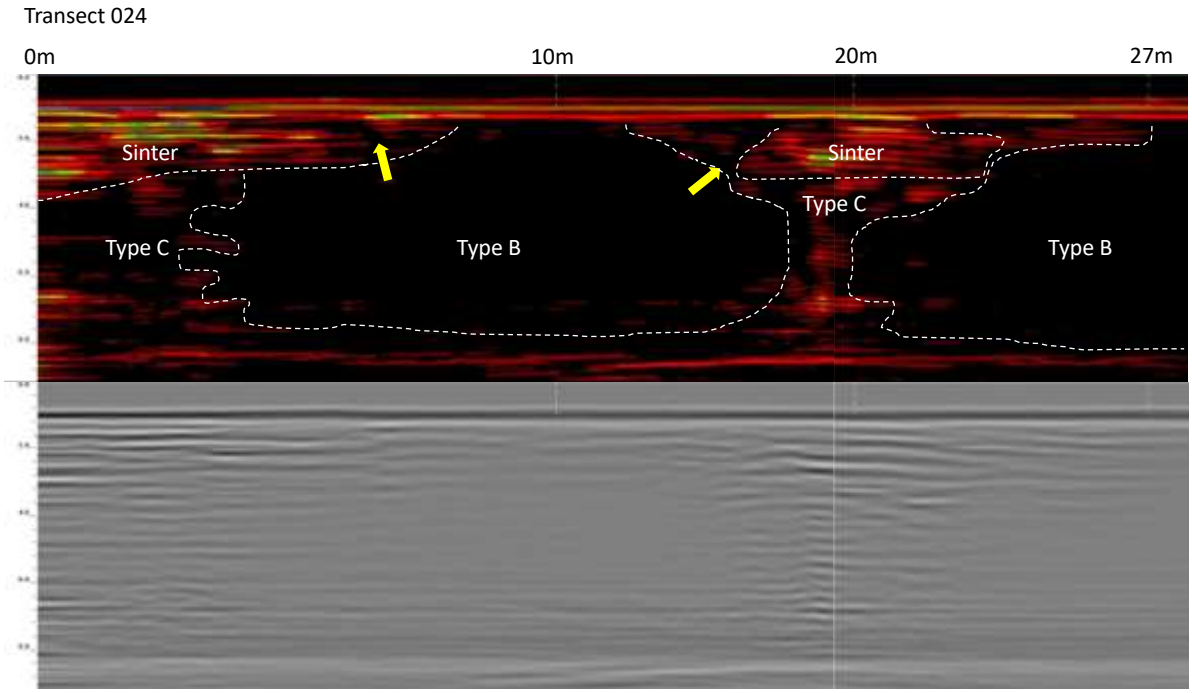

Figure 26: Transect 024. 27 m long profile. 2 m thick sinter sheet occurs from 0 to 7 m. Another sinter sheet of similar thickness is present from 17 to 23 m. Two vents within the sinter are shown by yellow arrows at 7 m and 17 m. Type B and Type C were imaged below the sinter.

7.21 Transect 025

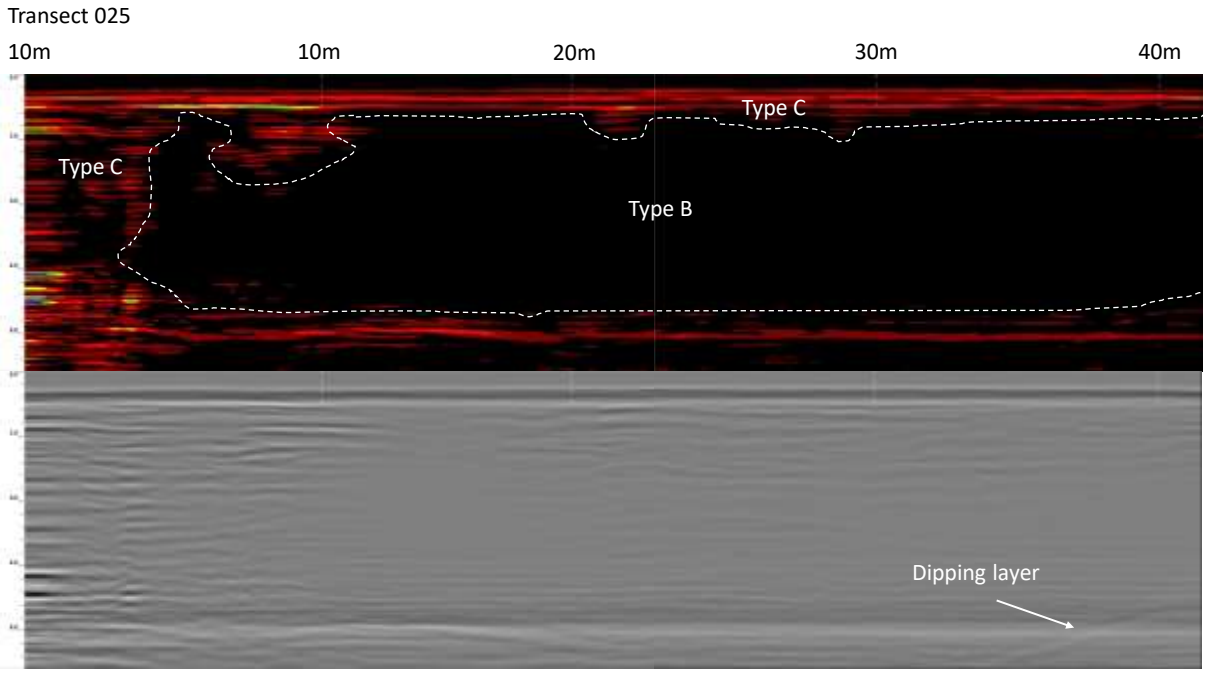

Figure 27: Transect 025. 40 m long profile. No sinter identified in this area. Type B dominates the profile with a thin layer of Type C above and below the Type B material. A dipping layer was identified in the transect.

7.22 Transect 026

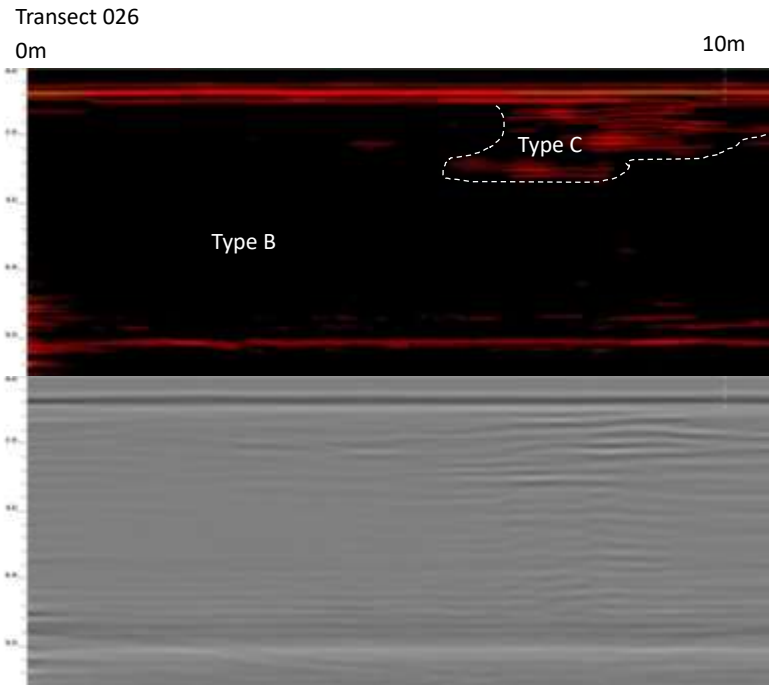

Figure 28: Transect 026. 10 m long profile. A small pocket of Type C occurs at 7 m to 10 m; the remaining area is composed of Type B.

7.23 Transect 027

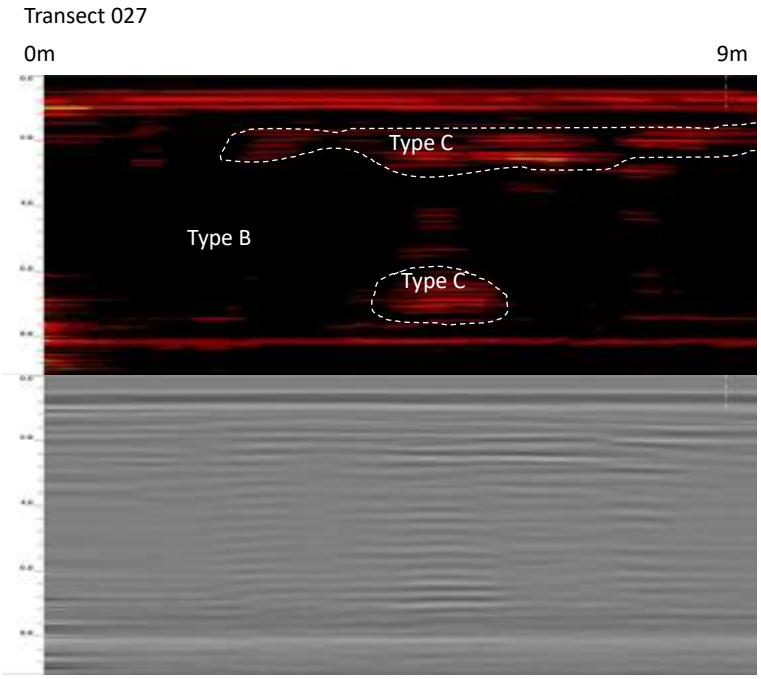

Figure 29: Transect 027. 9 m transect line. No strong sinter reflectors were imaged in this area. Small zones of Type C occur from 3 to 9 m, but the area is dominantly Type B.

7.24 Transect 028

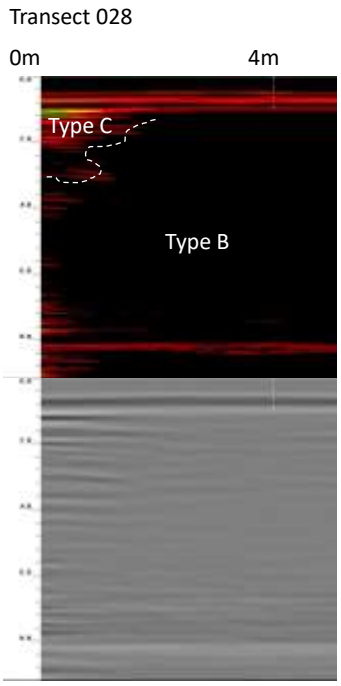

Figure 30: Transect 028. 4 m long profile. With the exception of a small section of Type C at the transect start, Type B is the only material identified.

7.25 Transect 029

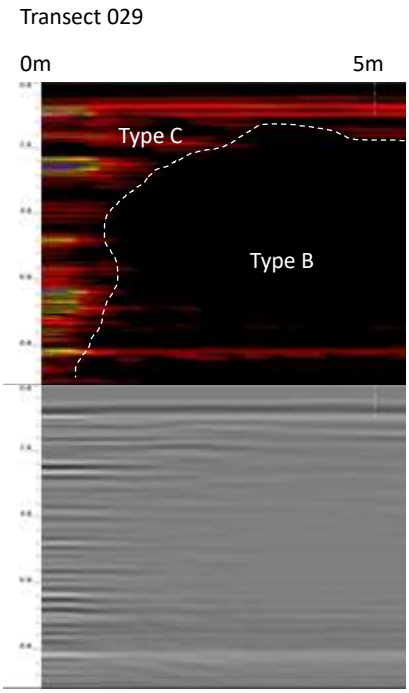

Figure 31: Transect 029. 5 m long profile. Type C dominates 0-1 to a depth of ~8 m. Type B was identified in the remaining area.

7.26 Transect 030

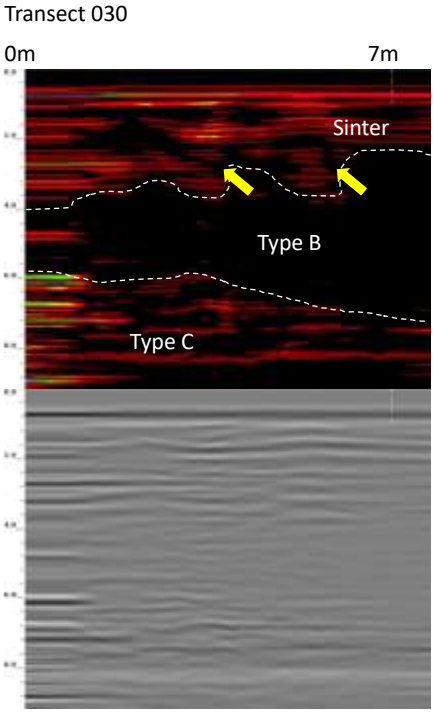

Figure 32: Transect 030. 7 m transect line. Sinter was identified along the transect line to a depth of ~ 4 m. Two fractures within the sinter with similar orientations are shown by the yellow arrows. Type B is immediately below the sinter, and Type C is below the Type B material.

7.27 Transect 031

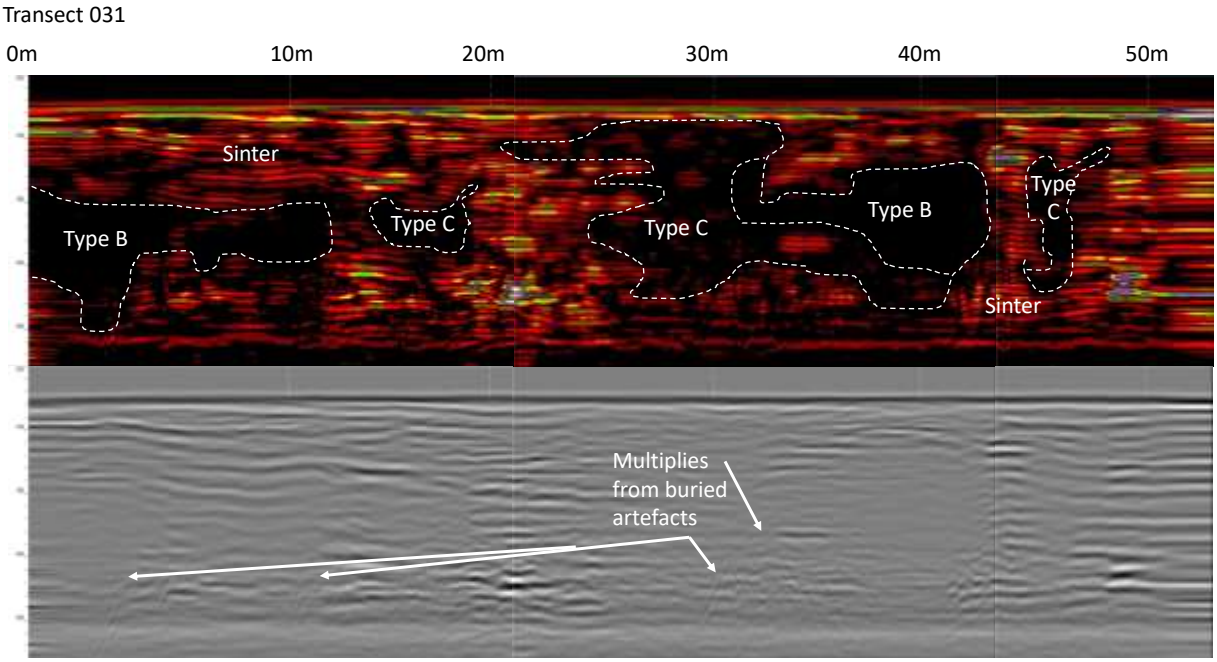

Figure 33: Transect 031. 50 m long profile. Thick, expansive sinter with five isolated areas of Type B and Type C embedded within the sinter. There are a series of strong hyperbolic reflectors indicating buried objects at ~5 m, 11 m, 16 m and 30 m to 37 m.

7.28 Transect 032

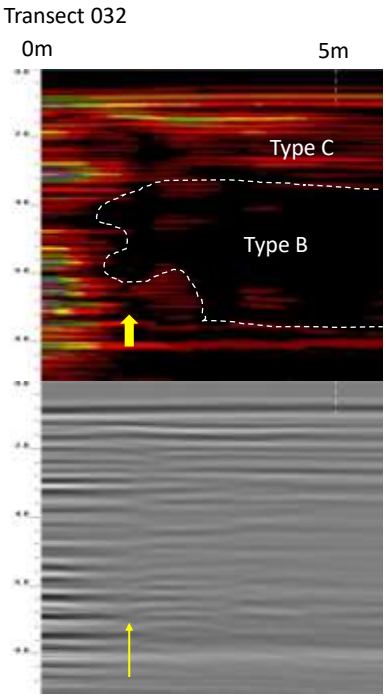

Figure 34: Transect 032. 5 m long profile. Type B and Type C material with a vent at ~1 m along the transect line, with a near-vertical orientation.

7.29 Transect 033

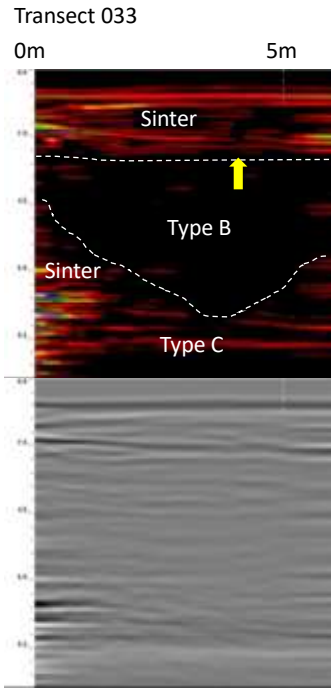

Figure 35: Transect 033. 5 m transect line. 2 m thick, sinter layer overlies Type B and Type C horizons along the entire profile. Sinter was also imaged at a depth of 5 to 8 m below Type B at the start of the transect.

7.30 Transect 034

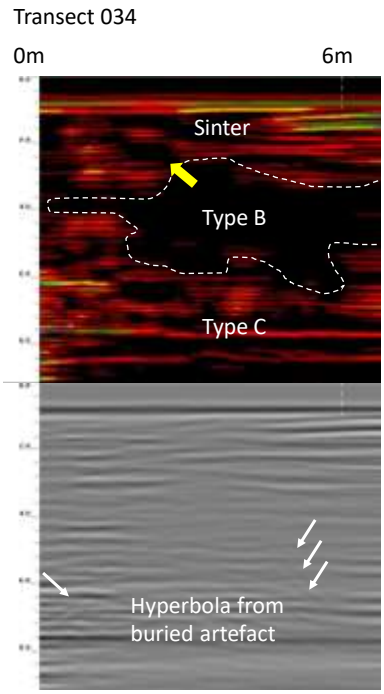

Figure 36: Transect 034. 6 m long profile. A 3.5 m thick sinter layer overlies Type B and Type C layers. Four reflections are generated by a buried object as shown by the hyperbolic nature of the returning radar wave.

7.31 Transect 035

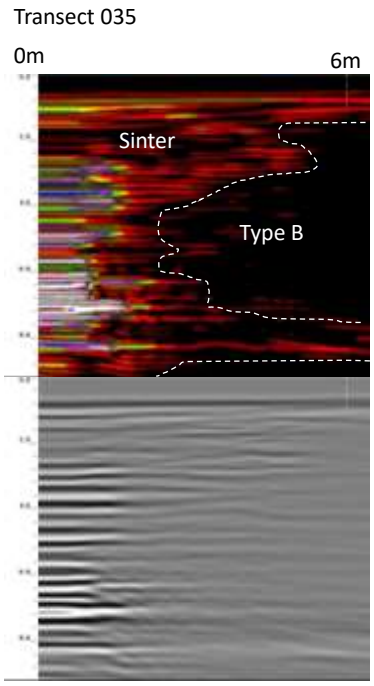

Figure 37: Transect 035. 6 m transect line. Sinter imaged near the surface and varies in thickness from ~1 to ~8 m. Type B is present below the sinter from ~3 to 6 m along the profile and varies in thickness.

7.32 Transect 036

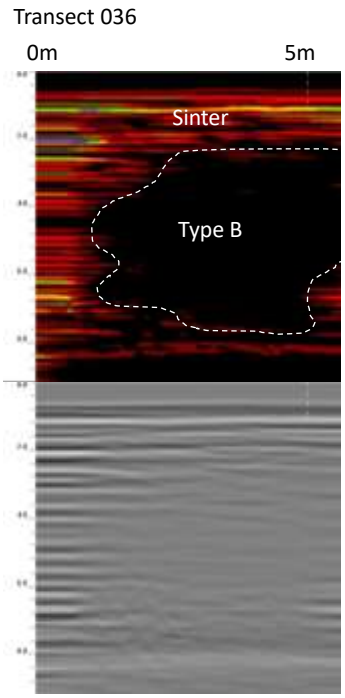

Figure 38: Transect 036. 5 m profile line. Continuous, horizontal layers of sinter occur to ~ 3 m depth along the entire transect. The sinter thickens to ~8 m at the start of the transect. Type B material was also imaged.

7.33 Transect 037

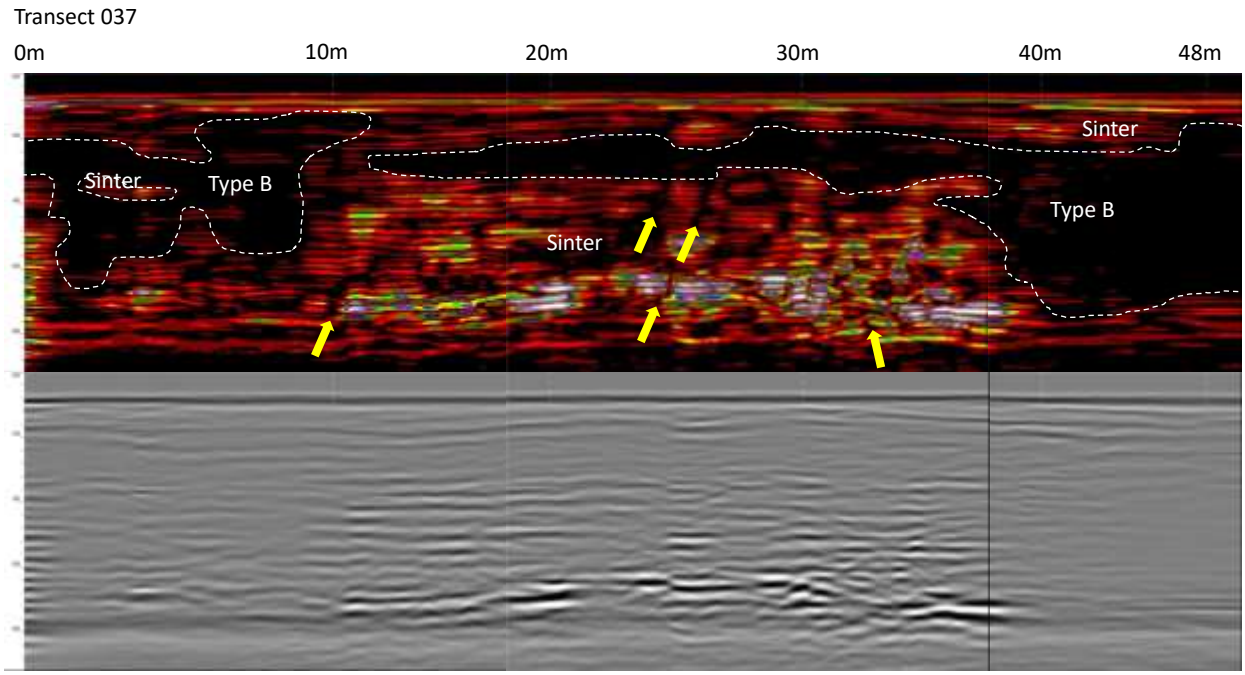

Figure 39: Transect 037. 48 m long profile. The majority of the transect area is sinter, with strong sinter reflections occurring at a depth 5 to 8 m, between the 10 to 37 m marks. Multiple vent pathways of similar orientation were imaged at 10 m, 25 m, 26 m and 33 m (yellow arrows). Discontinuous zones of Type B material occurs within the sinter areas.

7.34 Transect 038

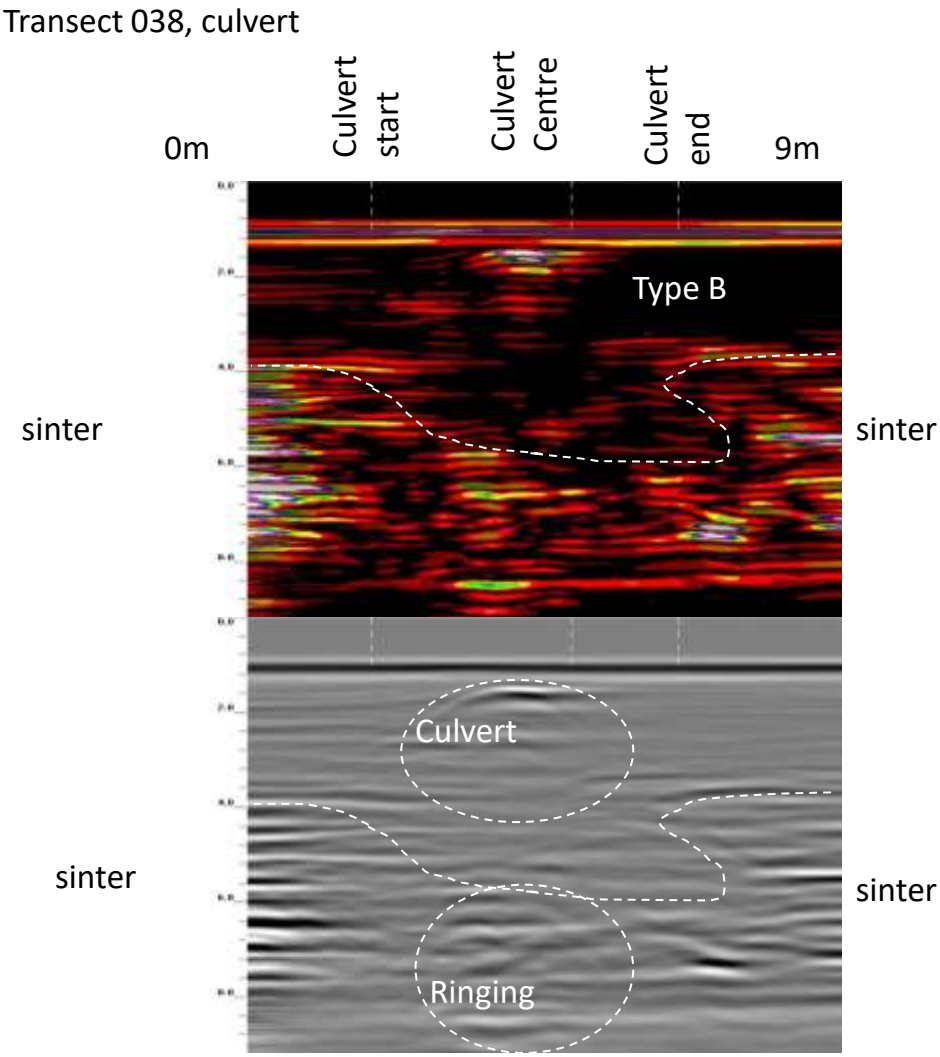

Figure 40: Transect 038. 9 m long profile. The upper 4 to 5 m depth is Type B. Sinter is imaged to the left and right below 4m depth. To the immediate left and right of the dotted white line designating both the culvert and ringing zones, images typical of saturated sub-surface conditions are visible. Given transect 038 is perpendicular to the topographic stream flow, it is possible these are subsurface water flow channels. It is not possible to tell from this image whether the possible flow pathways are naturally made or anthropogenic in nature. The culvert was identified by the hyperbolic reflections at the 4 m mark.

8 Sinter distribution map

Figure 41: Map showing the thickness and spatial distribution of sinters in the western side of the study area.

Figure 42: Map showing the thickness and spatial distribution of sinters in the eastern side of the study area.

9 Summary

The GPR study was successful in mapping sinters and subsurface features in the Armstrong Reserve area. Sinter was observed in the banks of the Onekeneke stream. Sinter in the area consists of multiple, near-horizontal layers. The thickest sinter (>6 m) occurs in the western section of the study area. The sinter is generally thinner in the eastern sections, and is less abundant. Minimal sinter was identified between the western and eastern zones of the area (transects 013, 017, 018 and 019).

Vents were easily distinguished in the areas with sinter. More vents were identified in the west than the east. Vents may exist in the Type B and Type C areas, but to identify them on GPR, it is necessary for them to have a contrasting radar signature to the surrounding material. Vents are recognisable when sinter (strong amplitude reflections) surrounds the vents (low amplitude reflections), but when the vents (low amplitude reflections) are surrounded by the low amplitude reflections of Type B and Type C material, there is no contrast to allow detection. The vents in the Armstrong Reserve may be extinct and infilled with soil. Alternatively, there may be minor steam ascending through the vents but we found no evidence of heat or steam discharge at the surface. A 1.5 m deep temperature survey would need to be undertaken to detect anomalous heat in the near sub-surface.

Culvert 1 (Eastern) was not dry at the time of the survey and therefore could not be imaged.

Culvert 2 (Western) was proposed to have a fractured sinter bed due to the installation of the culvert. No strong sinter reflectors were imaged on either side of the culvert at shallow depths (4 m). A potential sinter horizon was imaged below the base of the culvert, with strong reflectors at the south-western and north-eastern sides and weaker signatures in the middle. This weak signal return could be due to either; present-day or historic steam alteration, or present-day water saturation. There is also the possibility that the central faded area consists of another material (i.e., not sinter). However, this is less likely as the GPR reflections appear to be continuous along the profile. Ringing from the culvert pipe further complicates the interpretation directly under the culvert. Given Transect 038 lies perpendicular to the natural topographic water flow of the Onekeneke stream, it is probable that the central faded area imaged, is showing sub-surface water flow pathways. It is not possible from the GPR image to determine whether these potential flow paths beneath the culvert have formed by natural or anthropogenic means.

Geophysical data can have multiple interpretations, as various materials can share a similar signature. It is important to acknowledge that there are multiple interpretations that can be made off this data. Ground-truthing the area would be necessary to verify the interpretations made in this report.

10 Discussion

The Armstrong Reserve is located within the Wairakei-Tauhara geothermal system, which is dominated by northeast-southwest oriented fault structures (McNamara et al. 2016).

Cody (1993) documents extensive sinter terraces and discharging hot springs of the Waipahihi Valley in the mid-late 19th century, and concludes from anecdotal evidence that spring flow considerably reduced as a result of the 1931 Napier Earthquake of magnitude 7.9.

At Armstrong Reserve, historic sinter sheets are visible in the banks of the Onekeneke Stream, but no sinter outcrops occur in the Reserve. We imaged shallow fractures in the buried sinter at Armstrong Reserve. While orientations of individual fractures were variable, the zone where fractures were observed shows a northeast-southwest orientation which correlates to the regional structural trend in the Taupo area.

No cores were taken at Armstrong Reserve to ground truth the GPR data. However, GPR transects were collected along the banks of the Onekeneke Stream, over sites where sinter was visible. Previous GPR work in sinter areas show that sinter produces strong amplitude reflectors (Dougherty and Lynne, 2011; Lynne and Sim, 2012; Lynne and Smith, 2013; Lynne et al., 2015). Strong amplitude reflections occurred over the visible sinter in the banks of the Onekeneke Stream.

The results of the GPR survey suggest an expansive siliceous sinter terrace occurs beneath the present-day grassed area at Armstrong Reserve. GPR imaging reveals the western, central and eastern sections contain approximately 2000 m^2, 50 m^2 and 500 m^2 of buried sinter, respectively. For this quantity of sinter to have accumulated there must have been considerable and sustained discharge of alkali chloride water in the Armstrong Reserve area in the past.

11 Conclusion

GPR has proven successful in imaging buried sinter at Armstrong Reserve, as well as identifying fractures within the sinter. The application of GPR to identify buried, historic, siliceous sinter extends our ability to locate sites where alkali chloride water discharged at the surface in the past, but where no discharging hot springs occur today.

References/Bibliography

Cody, A. D.: Onekeneke Thermal Valley (De Brett's): A Summary of Available Historical Data. Hamilton, Waikato Regional Council. (1993).

Dougherty A.J., Lynne, B.Y.: Utilizing ground penetrating radar and infrared thermography to image vents and fractures in geothermal environments. Geothermal Resource Council Conference, San Diego, USA. *GRC Transactions*, volume 35, pp. 743-749. (2011).

Lynne, B.Y.**,** Sim, C.Y.: The successful application of Ground Penetrating Radar to image the opal-A to quartz diagenetic sequence in trace element-rich and trace element-poor sinters. *Geothermal Resource Council*, USA. (2012).

Lynne, B.Y., Smith, G.J.: A new investigative approach to understanding heat migration pathways within the shallow subsurface at Orakei Korako, New Zealand. *Geothermal Resource Council*, USA. v. 37. (2013).

Lynne, B.Y., Smith, I.J., Smith, G.S., Old Faithful Geyser, Yellowstone National Park, USA: Ground Penetrating Radar survey. *Geothermal Scientific Investigations Technical Report,* 83 p. (2015).

McNamara, D.D., Bannister, S., Villamor, P., Sepulveda, F., Milicich, S.D., Alcaraz, S., Massiot, C.: Exploring structure and stress from depth to surface in the Wairakei geothermal field, New Zealand. *Proceedings, 41st Workshop on Geothermal Reservoir Engineering, Stanford University,* SGP-TR-209. 11 p. (2016).

Rosenberg, M., Wallin, E., Bannister, S., Bourguignon, S., Sherburn, S., Jolly, G., Mroczek, E., Milicich, S., Graham, D., Bromley, C., Reeves, R., Bixley, P., Clotworthy, A., Carey, B., Climo, M., Links, F.: Tauhara Stage II Geothermal Project: Geoscience Report 2010/138. 318 p. (2010)

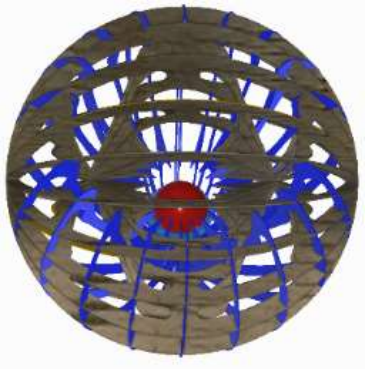

Appendix A - Ground Penetrating Radar report of Armstrong Reserve, Taupo, New Zealand: Photos, April 2016

Equipment

Figure 1: The Ground Penetrating Radar (GPR) unit imaged the subsurface using a 200 MHz GSSI antenna.

Figure 2: A SIR 3000 control module was used to collect GPR data.

Sinter

Figure 3: Sinter exposed in the stream.

Figure 4: Sinter exposed in the stream.

Figure 5: A view of the silica sinter rocks found at the stream.

Culvert

Figure 6: The culvert had a body of flowing water through it, making it impossible to scan with a GPR. The vegetation density and an uneven ground surface prevented GPR imaging.

Terrain complications

Figure 7: An overview photograph of the terrain encountered during the field trip. The long grass, blackberry vines and overgrown logs form the hummocky patches seen here and can restrict the placement of GPR transects.

Transect location photographs

Transect 005

Transect 006

Transect 007

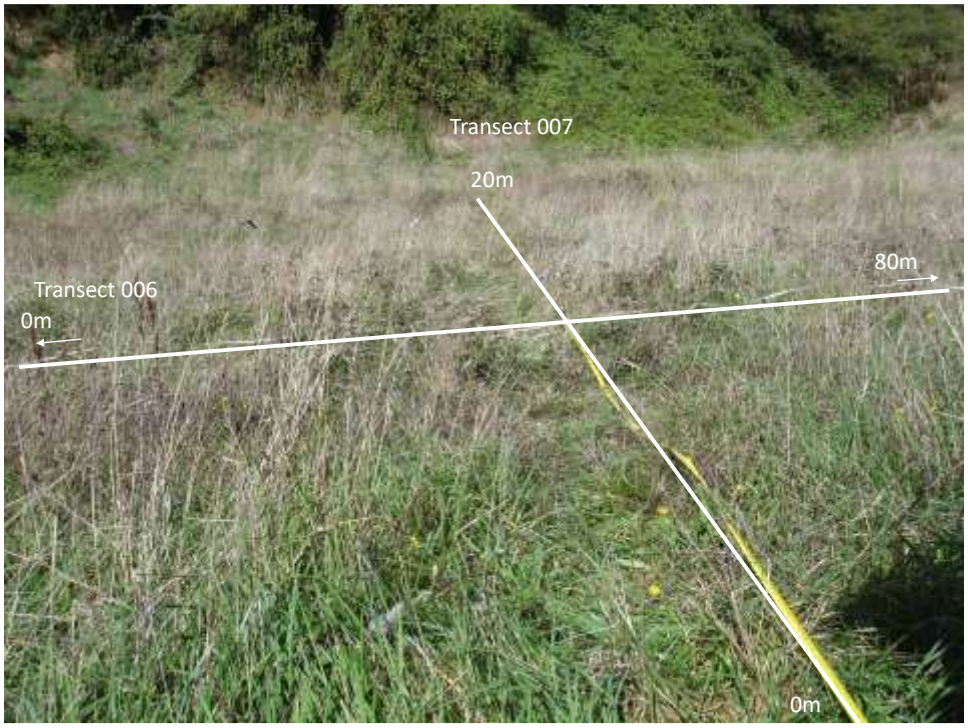

Transect 008

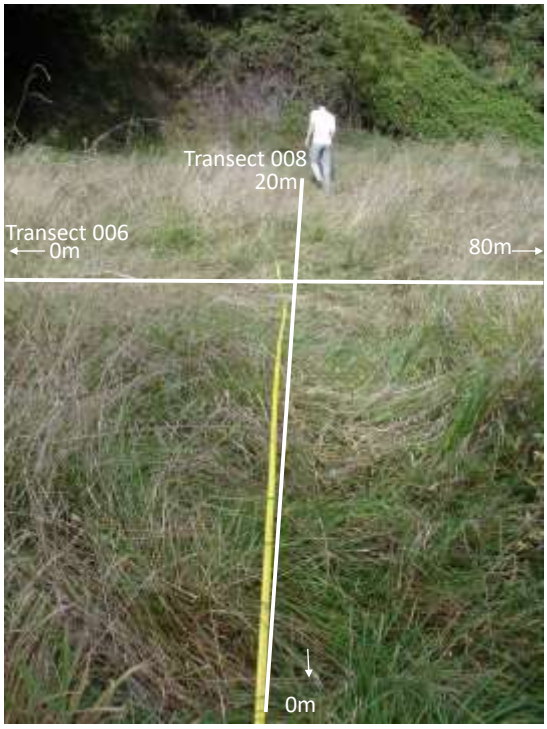

Transect 009

Transects 010 and 011

Transect 012 to 016

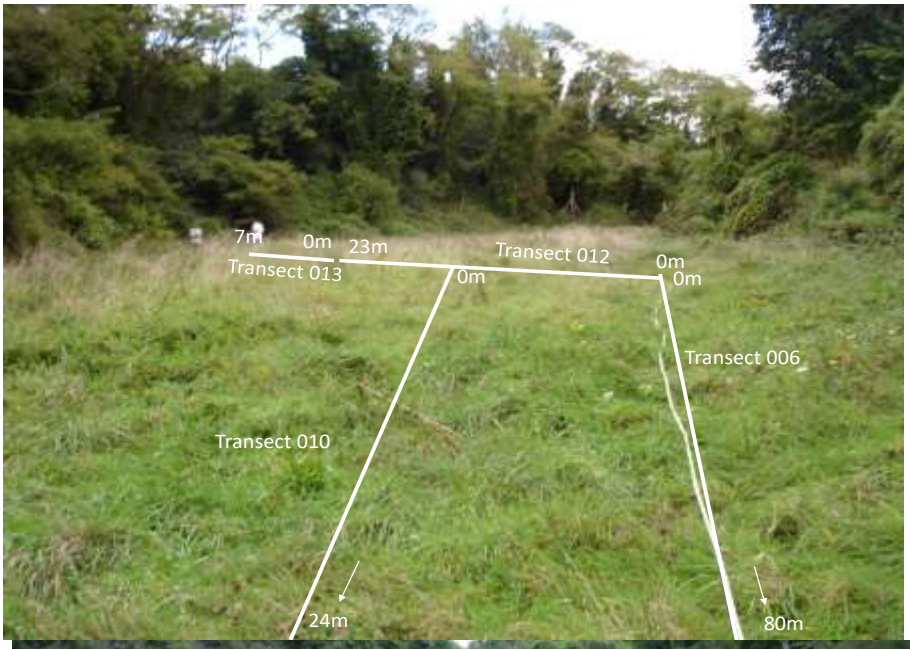

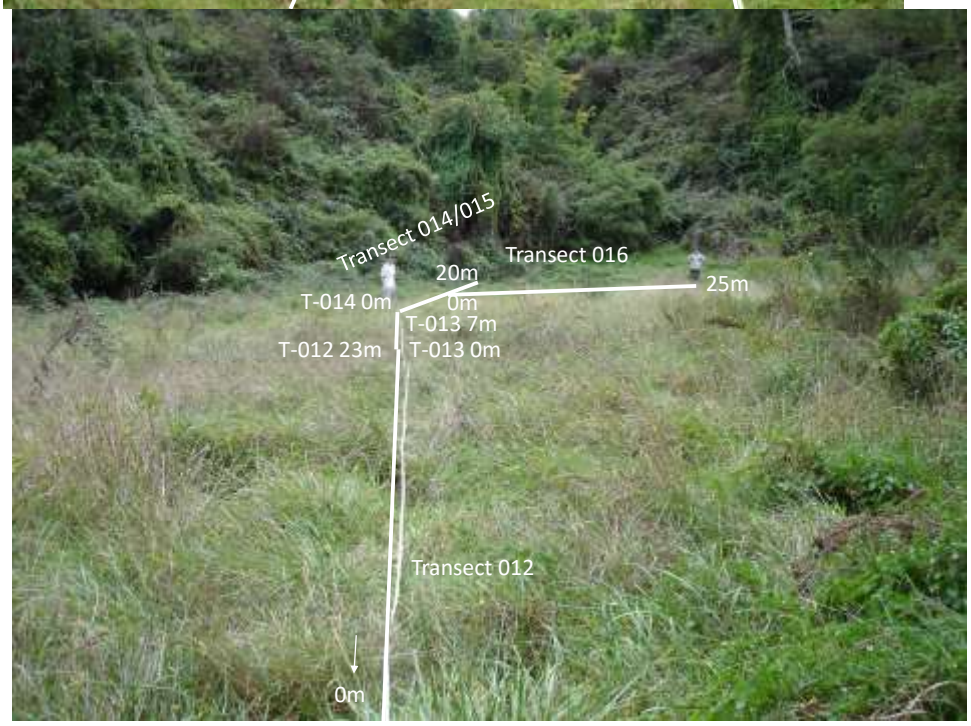

Transect 016

Transect 017

Transect 018

Transect 019

Transect 020 and 021

Transect 022 and 023

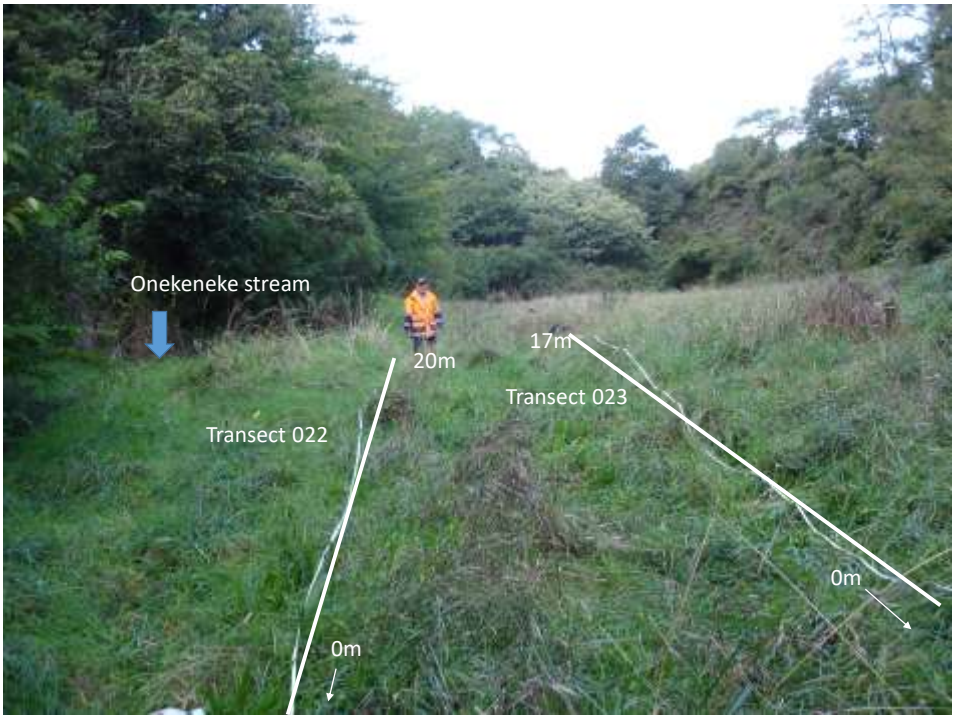

Transect 024 to 030

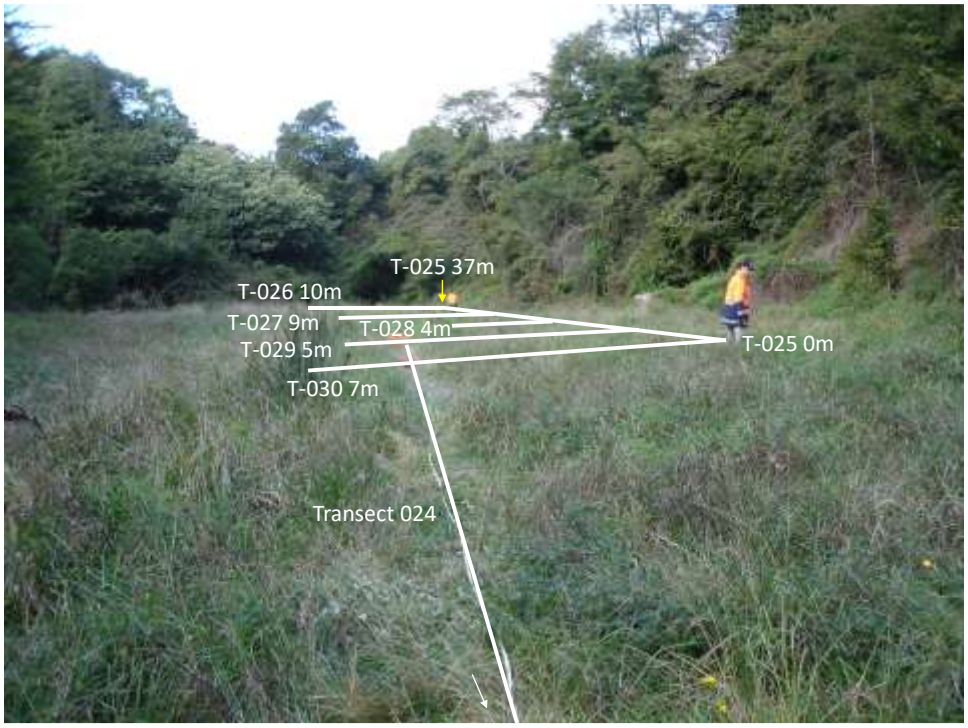

Transect 026

Transect 027

Transect 028

Transect 029

Transect 030

Transect 031 to 036

Transect 033

Transect 035

Transect 036

Transect 037

Transect 038